

Heat and Moisture in Wooden Bearings of Monuments

H.L. Schellen¹, M. Spierenburg², A.W.M. van Schijndel¹

1. Department Built Environment, Eindhoven University of Technology, Eindhoven, The Netherlands

2. DPA Cauberg-Huygen, Amsterdam, The Netherlands

Summary

Nowadays, thermal insulation is applied to most buildings. However, this proves to be a challenge for most monumental buildings. When insulation needs to be applied at the interior side of a building, thermal bridges are inevitable. Wooden beam ends beared in an external wall are an example of such a (hygro-)thermal bridge. Adding interior insulation introduces a risk of mold growth and can even lead to the deterioration of wood.

In this area several studies, including measurement studies, have already been performed. With the use of simulation models, however, the risk on deterioration of wooden beams can be analyzed making use of variant studies. A simulation model made with COMSOL multiphysics that uses the Logarithmic capillary pressure (L_{pc}) as moisture potential has been developed.

The goal of this research is to calculate the heat and moisture development at the wooden beam end within a monumental building. In the first place this will provide more knowledge about that specific detail. That may contribute to preserving wooden beams of monumental buildings in the future.

Second, the calculation itself is of scientific value. The calculations will be made in a state of the art simulation model in COMSOL. The accuracy of the COMSOL model using Logarithmic capillary pressure as moisture potential is determined by validating experiments from literature and comparison with Delphin software results. The COMSOL models have been validated with measurement results from literature (HAMSTAD). After the COMSOL and Delphin models have been compared in 1D, there weren't hardly any noticeable differences. Moreover, by adding more detail to this COMSOL model sophisticated multi-physics models are developed for future use.

Introduction

Applying thermal insulation to building envelopes is common for new built buildings. Old buildings built in the Netherlands before 1950, however, are mostly not applied with thermal insulation.

There is a risk of permanently damaging a monumental building when applying thermal

insulation in a wrong way. Therefore, studies are performed to see whether thermal insulation can be applied without damaging the building [Gnoth, S. 2005],[Holle, H.J. 2009],[Stopp, H. 2010],[Strangfeld, et al., 2011],[Grobbaauer & Ruisinger, 2012],[Kehl, D. 2012],[Morelli & Svendsen, 2012],[Guizzardi, M. 2015a].

[Kehl, D. 2013] describes that it is expected that the connection of wooden beams to stone walls is critical. A high moisture content is expected, certainly, when insulation is applied at the interior. The results show that this detail is not critical for buildings with external walls that have a repellent plaster or coating. For bare brick walls, however, this is indeed a critical detail.

In the Netherlands, bare brick walls are common. The connection of wooden beams to stone walls is present in most monumental buildings. Wooden beams are part of the construction, either as part of the floor or as part of the roof construction. It is only after about 1920 that concrete is being used as replacement for wood in the construction of floors and roof constructions and at that time only on a small scale.

The hygrothermal behavior of these details can be analyzed experimentally by measuring an existing situation. However, it is also possible to use simulation software to predict the hygrothermal behavior [Janetti, Ochs & Feist, 2011].

In the simulation software, a coupling of moisture and heat is made. The moisture part can be simulated with different potentials: p_c (capillary pressure), RH (relative humidity), w (water content) and L_{pc} (Logarithmic capillary pressure). Each of the potentials has its own advantages and disadvantages. [Portal, N.W., 2011] describe L_{pc} is the most suitable method for extreme situations at the boundaries. For this reason, modeling with L_{pc} as moisture potential continued [Uittenbosch, S. 2012].

In a comparison study between moisture potentials [Janssen, H. 2014] it is shown that L_{pc} might have worse results for near-saturation conditions, when compared to p_c and RH.

Theory

The Heat, Air and Moisture (HAM) transport mechanisms can be described through a set of equations. They originate from the basic principle that there is a balance in energy, moisture and air:

$$\frac{\partial E}{\partial t} = -\nabla \cdot (q_{cond} + q_{conv} + q_{moist})$$

$$\frac{\partial w}{\partial t} = -\nabla \cdot (g_{diff} + g_{adv} + g_{liq})$$

$$\varepsilon \frac{\partial \rho_a}{\partial t} = -\nabla \cdot (\rho_a \cdot r_a)$$

E = total enthalpy [J/m³]

w = water content [kg/m³]

T = temperature [K]

t = time [s]

q_{conf} = thermal flux [W/m²] analog to q_{conv} (convection) and q_{moist} (evaporation, condensation)

g_{diff} = vapour diffusion flux [kg/m²·s] analog to

g_{adv} (advection) and g_{liq} (liquid)

ρ_a = air density [kg/m³]

r_a = air flow rate [m/s]

ε = open porosity [-]

Heat

Heat transport in materials can be described by conductive and convective heat transport: [Berger, J. 2014]:

$$\frac{\partial E}{\partial t} = -\nabla \cdot (q_{cond} + q_{conv})$$

The internal energy within a material is present in three different forms. Energy of the dry material, energy as a combination where both air and water vapor are present and energy from water in liquid form.

The combination of air and water vapor is also known as the gaseous phase and is often neglected. Instead, the gaseous phase can be split into two parts. Then the calculation only consists of energy from the dry material and energy from the liquid [Hagentoft, C.E. 2004],[Berger, J. 2014],[Li, Q., 2009]:

$$\frac{\partial E}{\partial t} = (c_0 \rho_0' + c_1 w) \cdot \frac{\partial T}{\partial t} + c_1 T \cdot \frac{\partial w}{\partial t}$$

c₀ = specific heat capacity material [J/(kg·K)]

ρ₀ = specific density [kg/m³]

c₁ = specific heat capacity of liquid water [J/(kg·K)]

w = moisture content [kg/m³]

In this equation, the term

$$c_1 T \cdot \frac{\partial w}{\partial t}$$

represents driving rain [Berger, J. 2014].

Conductive heat is determined by the temperature gradient [Berger, J. 2014],[Hagentoft, C.E. 2004] [Delgado, J.M.P.Q. 2013]. Following Fourier's law the following equation can be used to determine conductive heat:

$$q_{cond} = -\lambda(w) \cdot \nabla T$$

λ(w) = thermal conductivity [W/(m·K)]

There is a difference in thermal conductivity depending on the type of material. Isotropic materials have an equal thermal conductivity in all directions of the material. Anisotropic materials like wood have thermal conductivity values that can differ depending on the direction of the heat flow [Vinha, J. 2007].

The thermal conductivity depends on the relative humidity and with that the moisture content inside the material. Also, the temperature of the material influences the thermal conductivity [Hagentoft, C.E. 2004],[Renato, P. 2013].

Convective heat is also represented in the energy balance equation. Convective heat transfer consists of three flow mechanisms: the liquid flow and vapor flow - both influenced by moisture - and the dry air flow, which is only influenced by air transfer [Li, Q. 2009],[Santos, G.H. 2009].

When the liquid flow, vapor flow and dry air flow are combined the following equation is obtained:

$$q_{conv} = \underbrace{L_v \cdot \nabla (\delta_p \nabla p_v)}_{\text{liquid flow}} - \underbrace{L_v \cdot r_a \cdot \rho_v}_{\text{vapour flow}} - \underbrace{r_a \cdot \rho_a \cdot c_{p,a}}_{\text{dry air flow}} \cdot \nabla T$$

L_v = enthalpy of evaporation/condensation (latent heat) [J/kg]

ρ_v = water vapor density [kg/m³]

p_v = water vapor pressure [Pa]

δ_p = vapor permeability of the material [kg/m·s·Pa]

r_a = air flow rate [m/s]

ρ_a = density of dry air [kg/m³]

c_{p,a} = specific heat of dry air [J/kg·K]

External boundary conditions:

Both heat transfer and moisture transfer in building constructions depend on the internal conditions and the conditions of the environment around the material.

Aside from the similarities there are also differences. Commonly, moisture transfer through a construction is a process of weeks or months. Heat transfer through the same construction, however, is

commonly a process of hours or days. The difference in duration of these processes is important.

Daily temperature fluctuations reach further into the construction than daily moisture fluctuations. However, a change in temperature also affects the relative moisture levels in the materials [Woloszyn, M. 2008]. Internal or external condensation can occur due to temperature changes. Even when the moisture levels in the material are unchanged.

It is possible to calculate the boundary conditions for heat using different equations. In this study, the equation from [Li, Q. 2009] is used as a starting point:

$$q_e = \underbrace{h_e \cdot (T^{eq} - T_s)}_{\text{heat from air \& radiation}} + \underbrace{L_v \cdot \beta_e \cdot (p_{v,e} - p_{v,s})}_{\text{latent heat}} + \underbrace{g_l \cdot c_l \cdot T_e}_{\text{heat from rain}}$$

β_e = surface moisture transfer coefficient [kg/m²·s·Pa]

$p_{v,e}$ = water vapour pressure of outdoor air [Pa]

$p_{v,s}$ = water vapour pressure at surface [Pa]

g_l = mass flux of liquid water [kg/m²·s]

$c_{p,l}$ = specific heat of liquid water [J/kg·K]

h_e = heat transfer coefficient outdoor [W/m²·K]

T_{eq} = equivalent exterior temperature [K] (combines air temperature, solar radiation and long wave radiation).

T_s = temperature of surface [K]

T_e = temperature of outdoor air [K]

Internal boundary conditions:

The analogy between the moisture boundary conditions and the heat boundary conditions also applies to the internal conditions. The equation to calculate the internal boundary conditions is less complex than the equation of the external boundary conditions, due to the precipitation term that is left out and the indoor air temperature (T_i) that replaces the T_{eq} term [Li, Q. 2009].

$$q_i = h_i \cdot (T_i - T_s) + L_v \cdot \beta_i \cdot (p_{v,i} - p_{v,s})$$

h_i = heat transfer coefficient of interior [W/m²·K]

T_i = interior temperature [K]

Moisture

Moisture transfer consists of two physical phenomena, the flux of vapor and the flux of liquid water respectively.

The moisture part can be simplified into the following form [Berger, J. 2014] [Hagentoft, C.E. 2004]:

$$\frac{\partial w}{\partial t} = -\nabla \cdot (g_v + g_l)$$

w = moisture content [kg/m³]

g_v = mass flux of vapor [kg/m²·s] (contains both

diffusion and advection)

g_l = mass flux of liquid water [kg/m²·s]

Vapor flux:

The vapor flux can be depicted with Fick's law [Berger, J. 2014],[Hens, H.L.S.C. 2015],[Portal, N.W. 2011]:

$$g_v = -\frac{1}{\mu} \frac{D_v}{R_v T} \cdot \nabla p_v + r_a \cdot \nabla \rho_v$$

Here μ is a function depending on the moisture content.

The vapor pressure can be determined according to Kelvin's law. This law describes the relation between vapor and liquid [Berger, J. 2014],[Wit, M. 2009].

$$p_v = p_{sat} \cdot \exp\left(\frac{p_c}{\rho_w R_v T}\right)$$

p_{sat} = saturation pressure [Pa]

p_c = capillary pressure [Pa]

ρ_w = density of the liquid phase (water) [kg/m³]

R_v = gas constant for water vapor [J/kg·K]

The vapor diffusion coefficient in air (D_v) can be calculated with an empirical function.

Both [Renato, P. 2013] and [Börjesson, F. 2013] use the simplified function from Schirmer:

$$D_v = 2.31 \cdot 10^{-5} \frac{p_0}{p_a} \left(\frac{T}{273}\right)^{1.81}$$

p_0 = Standard ambient pressure [Pa]

p_a = Ambient air pressure [Pa]

Liquid transport:

If vertical suction is not present, the gravitational part can be left out and the following equation is obtained [Berger, J. 2014],[Delgado, J.M.P.Q. 2013],[Hagentoft, C.E. 2004]:

$$g_l = -k_l(w) \cdot \nabla p_c$$

k_l = liquid permeability [s]

w = moisture content [kg/m³]

p_c = capillary pressure [Pa]

The capillary pressure can be determined using Young-Laplace's law [Berger, J. 2014]:

$$p_c = -\frac{2\sigma \cos \theta}{r}$$

θ = contact angle [°]

σ = surface tension [J/m²]

r = radius of capillar [m]

External boundary conditions:

Previous equations describe the behavior of moisture inside porous materials. In some equations the influence of the environment outside the materials is more or less included. However,

an equation solely describing transfer of moisture at the boundaries of the material has not been mentioned before. These boundary conditions are of great importance, since moisture entering and leaving the material determines the total amount of moisture inside the material.

The following equation is used to calculate the transfer at the surface [Vinha, J. 2007],[Santos, G.H. 2009],[Portal, N.W. 2011],[Vereecken, E. 2015] [Delgado, J.M.P.Q. 2015]:

$$g_e = \beta_e (p_{v,e} - p_{v,s}) + r_a \cdot \rho_v + R$$

g_e = flow density [kg/m²·s]

β_e = surface moisture transfer coefficient [kg/m²·s·Pa]

$p_{v,s}$ = water vapour concentration air at surface [Pa]

$p_{v,e}$ = water vapour concentration in ambient air [Pa]

r_a = air flow rate [m/s]

R = rain at surface [kg/m²·s]

The surface moisture transfer coefficient (β) is difficult to determine [Janssen, H. 2007]. Therefore, it can be calculated according to the Lewis analogy, which describes the relation between the heat and moisture transfer coefficient [Janssen, H. 2007],[Li, Q, 2009],[Vereecken, E. 2015],[Goesten, S. 2016]:

$$\beta_e = 7.7 \cdot 10^{-9} \cdot h_{c,e}$$

$h_{c,e}$ = convective heat transfer coefficient [W/m²·K]

The ratio of the molar masses is combined with the ratio of water vapor and air pressure resulting in the following equation [Janetti, M.B. 2016]:

$$\rho_v = \frac{M_v}{M_a} \cdot \frac{p_v}{p_a}$$

With $M_v = 0.018$; $M_a = 0.029$ and the p_a at 20°C with an absolute pressure of 1 atm = 101325. The upper equation results in the following [Wit, M. 2009] [Janetti, M.B. 2016]:

$$\rho_v = \frac{0.018}{0.029} \cdot \frac{p_v}{101325} = 0.6125 \cdot 10^{-5} \cdot p_v$$

The precipitation at a surface (R) depends on two components. The amount of rain coming down at a horizontal surface and the amount of rain that experiences a horizontal displacement caused by wind [Janssen, H. 2007]:

$$R = R_h \cdot \cos(\theta_v) + R_{wdr}$$

R_h = rain through a horizontal plane [kg/m²·s]

R_{wdr} = wind-driven rain [kg/m²·s]

θ_v = angle between horizontal plane and driving rain [°]

Internal boundary conditions:

The internal conditions at the boundaries are less complex than the external conditions, since rain

is not present [Vinha, J. 2007],[Santos, G.H. 2009],[Li, Q. 2009],[Portal, N.W. 2011],[Vereecken, E. 2015],[Delgado, J.M.P.Q. 2015].

The internal boundary conditions can be calculated with the following equations when air enters the structure

respectively in case air exits the structure:

$$g_i = \beta_i (p_{v,e} - p_{v,s}) + r_a \cdot \rho_v$$

$$g_i = \beta_i (p_{v,i} - p_{v,s}) + r_a \cdot \rho_v$$

β_i = surface moisture transfer coefficient [kg/m²·s·Pa]

The indoor surface transfer coefficient can be calculated according the Lewis analogy [Li, Q. 2009] with the following equation:

$$\beta_i = 7.7 \cdot 10^{-9} \cdot h_{c,i}$$

$h_{c,i}$ = convective heat transfer coefficient [W/m²·K]

Simulation Results

The COMSOL model was validated for a 1D construction and a 2D construction. The COMSOL model is validated with measurements performed by Harrestrup, M. [2016]: The original construction consists of a masonry wall with a thickness of 2 bricks (see figure 1). The load bearing beam inside the wall has a diameter of 150x150mm. The floor beam has a height of 140mm and is surrounded by an air layer of 20mm. The cladding and the plaster are both 30mm thick.

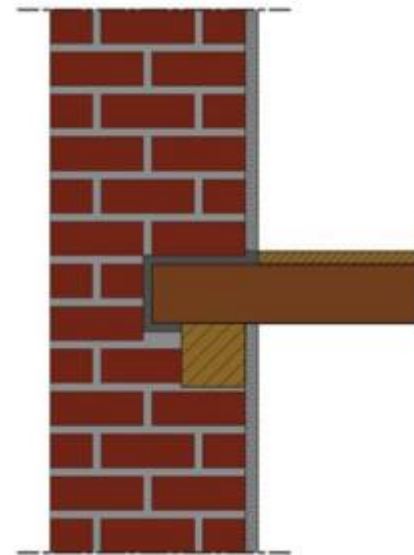


Figure 1. Danish construction used by [Harrestrup, M. 2016].

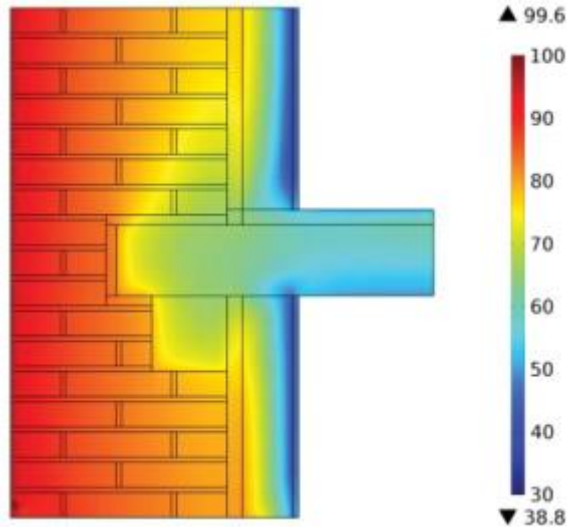


Figure 2. RH distribution within the construction during a rain event at 29-12-2012.

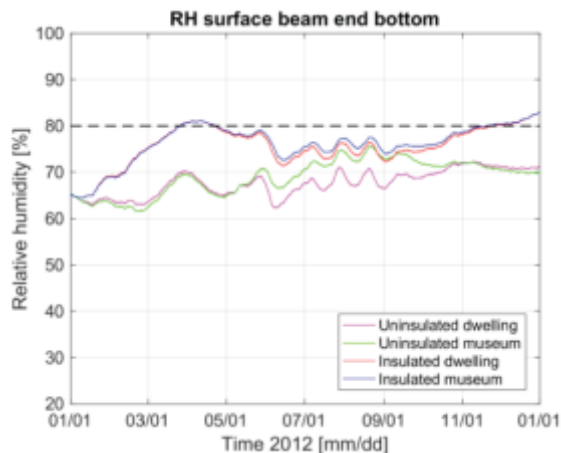


Figure 3. RH at the surface of the wooden beam end. The uninsulated situation with a dwelling (magenta) and museum (green) indoor climate is compared to the insulated situation with dwelling (red) and museum (blue) indoor climate.

Conclusions

Accuracy of the COMSOL model using Logarithmic capillary pressure as moisture potential and the differences between different moisture potentials. Simulations with COMSOL multiphysics are validated in 1D with Delphin. In the COMSOL model logarithmic capillary pressure (Lpc) is used as moisture potential, while the Delphin model uses capillary pressure (pc) as potential. Using similar input variables, both models produced equal results for Heat, Moisture and Air transport - RMSE remains below 1% -.

After this 1D validation, the COMSOL model is used for a comparison with temperature and relative

humidity measurements in a wooden beam end connected to a wall. These measurements are performed by Harrestrup, M. [2016]. For the temperature, the results from the model and measurements differed $<8^{\circ}\text{C}$ and for the relative humidity $<10\%$.

References

- Berger, J., Chhay, M., Guernouti, S. & Woloszyn, M. (2014). Proper generalized decomposition for solving coupled heat and moisture transfer. *Journal of Building Performance Simulation*, DOI: 10.1080/19401493.2014.932012.
- Börjesson, F. (2013). An investigation of the water vapour resistance. Chalmers University of Technology. Gothenburg, Sweden.
- Delgado, J.M.P.Q., Barreira, E., Ramos, N.M.M & Freitas, V.P. (2013). Hygrothermal numerical simulation tools applied to building physics. DOI 10.1007/978-3-642-35003-0.
- Gnoth, S., Jurk, K., & Strangfeld, P. (2005). *Hygrothermisches Verhalten eingebetteter Holzbalkenköpfe im innengedämmten Außenmauerwerk*. *Bauphysik* 27, Vol. 2. pp. 117-128.
- Grobbauer, M., & Ruisinger, U. (2012). *Innendämmung, Holzbalkenköpfe und Kastenfenster in der Sanierung*. Technische Universität Graz, *Bauphysiktagung 2012*. pp. 88-108. DOI: 10.3217/978-3-85125-237-8.
- Guizzardi, M., Derome, D., Vonbank, R. & Carmeliet, J. (2015a). Hygrothermal behavior of a massive wall with interior insulation during wetting. *Building and Environment*, Vol. 89. pp. 59-71.
- Hagentoft, C.E., et al. (2004). Assessment method of numerical prediction models for combined Heat, Air and Moisture transfer in building components: Benchmarks for one-dimensional cases. *Journal of thermal environment & building science*, Vol. 27, pp. 327-352. DOI:0.1177/1097196304042436.
- Hens, H.L.S.C. (2015). Combined heat, air, moisture modelling: A look back, how, of help? *Building and Environment*, Vol. 91. pp. 138-151
- Goesten, S. (2016). *Hygrothermal simulation model: Damage as a result of insulating historical buildings*. Master thesis.
- Harrestrup, M. & Svendsen, S. (2016). Internal insulation applied in heritage multi-storey buildings with wooden beams embedded in solid masonry brick façades. *Building and Environment*, Vol. 99. pp. 59-72.
- Holle, H.J. (2009). *Innendämmung bei erhaltenen Fassaden - ein baukonstruktives Projektbeispiel*. *Bauphysik* 31, Vol.

4. pp. 227-234. DOI: 10.1002/bapi.200910030.
- Janetti, M.B., Ochs, F. & Wolfgang, F. (2012). On the conservation of mass and energy in hygrothermal numerical simulation with COMSOL multiphysics. Proceedings of BS2013: 13th Conference of International Building Performance Simulation Association, Chambéry, France, August 26-28. pp. 2860-2867.
- Janssen, H. (2014). Simulation efficiency and accuracy of different moisture transfer potentials. *Journal of Building Performance Simulation*. Vol. 7, No. 5. pp. 379-389. DOI: 10.1080/19401493.2013.852246.
- Kehl, D. (2012). Holzbalkenköpfe im Mauerwerk. *Holzbau* 6. pp. 20-25.
- Kehl, D., Ruisinger, U., Plagge, R., & Grunewald, J. (2013). Wooden beam ends in masonry with interior insulation – A literature review and simulation on causes and assessment of decay. Proceedings of 2nd Central European Symposium on Building Physics.
- Li, Q., Rao, J., & Fazio, P. (2009). Development of HAM tool for building envelope analysis. *Building and Environment*. Vol. 44. pp. 1065–1073.
- Morelli, M., & Svendsen, S. (2012). Investigation of interior post-insulated masonry walls with wooden beam ends. *Journal of building physics* 36, Vol. 3. pp. 265-292. DOI: 10.1177/1744259112447928.
- Portal, N.W., Schijndel, A.W.M., & Kalagasidis, A.S. (2013). The multiphysics modeling of heat and moisture induced stress and strain of historic building materials and artefacts. *BUILD SIMUL*. Vol. 7. pp. 217–227. DOI: 10.1007/s12273-013-0153-4.
- Renato, P. (2013). Innovative approaches for the experimental determination of the liquid water conductivity and validation of a model for heat and moisture transfer in porous building materials.
- Santos, G.H., Mendes, N. & Philippi, P.C. (2009). A building corner model for hygrothermal performance and mould growth risk analyses. *International Journal of Heat and Mass Transfer*. Vol. 52. pp. 4862–4872.
- Stopp, H., Strangfeld, P., Toepel, T., & Anlauff, E. (2010). Messergebnisse und bauphysikalische Lösungsansätze zur Problematik der Holzbalkenköpfe in Außenwänden mit Innendämmung. *Bauphysik* 32, Vol. 2. pp. 61-72. DOI: 10.1002/bapi.201010008.
- Strangfeld, P., et al. (2011). Bauphysikalisch schadensfreie Innendämmung von Außenwänden mit eingebundenen Holzbalkenköpfen. *Wissenschaftstage der Hochschule Lausitz*.
- Uittenbosch, S. (2012). Risico van inwendige condensatie in een externe scheidingsconstructie. Eindhoven University of Technology.
- Vereecken, E., & Roels, S. (2015). Capillary active interior insulation: do the advantages really offset potential disadvantages? *Materials and Structures*. Vol. 48. pp. 3009–3021. DOI: 10.1617/s11527-014-0373-9.
- Vinha, J. (2007). Hygrothermal performance of timber-framed external walls in Finnish climatic conditions. Tampere University of Technology.

Appendix

Table 1: Material properties used for the COMSOL simulations

Material properties	Unit	Masonry	Lime mortar	Lime plaster	Spruce (wood)	Gypsum board	EPS	XPS
Density	[kg/m ³]	1788	1568	1800	528	850	23	35
Specific heat capacity	[J/kg·K]	868	1000	850	2000	850	1500	1500
Thermal conductivity	[W/m·K]	0.91	0.70	0.82	0.13	0.20	0.036	0.027
Water vapour resistance	[-]	13.2	30	12	40	10	96	225
Liquid permeability	[kg/m·s·Pa]	1.4·10 ⁻⁸	6.5·10 ⁻¹⁰	2.8·10 ⁻⁹	4·10 ⁻⁹	6.3·10 ⁻⁹	-	-
Air permeability*	[kg/m·s·Pa]	5·10 ⁻¹⁰	1.5·10 ⁻⁹	1·10 ⁻¹¹	5·10 ⁻¹¹	4.16·10 ⁻⁹	1.1·10 ⁻⁸	-

* Properties based at measurements from ASHRAE RP1018